applied sciences

MDPI

Article

Parameter Identification of Photovoltaic Cell Model Using Modified Elephant Herding Optimization-Based Algorithms

Amer Malki [1], Abdallah A. Mohamed [1,2], Yasser I. Rashwan [3], Ragab A. El-Sehiemy [4,*] and Mostafa A. Elhosseini [3,*]

1 College of Computer Science and Engineering, Taibah University, Yanbu 46421, Saudi Arabia; asamalki@taibahu.edu.sa (A.M.); aammohamed@taibahu.edu.sa (A.A.M.)
2 Mathematics and Computer Science Department, Faculty of Science, Menoufia University, Shebin El Kom 32511, Egypt
3 Computers and Control Systems Engineering Department, Faculty of Engineering, Mansoura University, Mansoura 35516, Egypt; yasser_e2005@hotmail.com
4 Electrical Engineering Department, Faculty of Engineering, Kafrelsheikh University, Kafrelsheikh 33516, Egypt
* Correspondence: elsehiemy@eng.kfs.edu.eg (R.A.E.-S.); Melhosseini@ieee.org (M.A.E.)

Abstract: The use of metaheuristics in estimating the exact parameters of solar cell systems contributes greatly to performance improvement. The nonlinear electrical model of the solar cell has some parameters whose values are necessary to design photovoltaic (PV) systems accurately. The metaheuristic algorithms used to determine solar cell parameters have achieved remarkable success; however, most of these algorithms still produce local optimum solutions. In any case, changing to more suitable candidates through elephant herd optimization (EHO) equations is not guaranteed; in addition, instead of making parameter α adaptive throughout the evolution of the EHO, making them adaptive during the evolution of the EHO might be a preferable choice. The EHO technique is used in this work to estimate the optimum values of unknown parameters in single-, double-, and three-diode solar cell models. Models for five, seven, and ten unknown PV cell parameters are presented in these PV cell models. Applications are employed on two types of PV solar cells: the 57 mm diameter RTC Company of France commercial silicon for single- and double-diode models and multi-crystalline PV solar module CS6P-240P for the three-diode model. The total deviations between the actual and estimated result are used in this study as the objective function. The performance measures used in comparisons are the RMSE and relative error. The performance of EHO and the proposed three improved EHO algorithms are evaluated against the well-known optimization algorithms presented in the literature. The experimental results of EHO and the three improved EHO algorithms go as planned and proved to be comparable to recent metaheuristic algorithms. The three EHO-based variants outperform all competitors for the single-diode model, and in particular, the culture-based EHO (CEHO) outperforms others in the double/three-diode model. According the studied cases, the EHO variants have low levels of relative errors and therefore high accuracy compared with other optimization algorithms in the literature.

Keywords: metaheuristics; solar cell systems; elephant herding optimization; alpha tuned EHO; cultural-based; biased initialization; parameter identification; single diode; double diode; three diodes

Citation: Malki, A.; Mohamed, A.A.; Rashwan, Y.I.; El-Sehiemy, R.A.; Elhosseini, M.A. Parameter Identification of Photovoltaic Cell Model Using Modified Elephant Herding Optimization-Based Algorithms. *Appl. Sci.* **2021**, *11*, 11929. https://doi.org/10.3390/app112411929

Academic Editor: Edris Pouresmaeil

Received: 10 November 2021
Accepted: 13 December 2021
Published: 15 December 2021

1. Introduction

Energy is an essential component of the universe and is considered one of the forms of existence. Energy is divided into two main types (renewable energy and non-renewable energy); non-renewable energy as fossil fuels has a terrible impact on the environment. Therefore, many nations tend to use renewable energy to produce their electricity. Solar energy is one of the primary and available renewable energy sources on the planet that has no pollution and easy installation as well as being inexpensive and noise-free. The need to add renewable energy sources is increased with the dramatic changes in electricity requirements. Therefore, the effective modeling of renewable energy resources is an important issue for efficient energy management [1].

Solar cells are one of the ways to take advantage of solar energy, so significant attention went to model photovoltaic (PV) cells [2–7]. Several parameters define the nonlinear electrical model of a solar cell, which must be studied in depth to design PV systems. It is vital to understand the current–voltage graph (I-V) before using PV cells. In addition to determining PV's parameters, picking a few points from this curve can also help. Based on the number of diodes, different parameter models are presented. Three different types are available: single diode, double diode, and three diode [8–11].

Parameter identification can be accomplished in two ways, using deterministic methods or using metaheuristics. Examples of traditional approaches are Lambert W-functions [12] and the interior-point method [13]. Although traditional models can solve parameter identification, it has some drawbacks facing nonlinear problems such as sensitivity to the initial solution besides sticking in a local optimum solution with heavy computations and taking a long time to reach this optimum. Therefore, metaheuristics algorithms are used to overcome these drawbacks. Examples of these metaheuristics are the Particle Swarm Optimization (PSO) [6], Genetic Algorithm (GA) [14], Differential Evolution (DE) [15], Harmony Search (HS) [16], Artificial Bee Colony (ABC) [17], and Simulated Annealing (SA) [18].

The continuous development in optimization methods has been notable in recent decades. For example, several optimization methods were developed and applied for different power system problems, as presented in [19,20]. Furthermore, in [21–25], an algorithm that mimics the elephant herding behavior called Elephant Herding Algorithm (EHO) was proposed for different applications. Reference [26] proposes three improved variants of EHO that are developed.

The basic architecture of the PV cell guarantees that two differentially doped semiconductor layers form a PN junction. When irradiation is present, the cell absorbs photons from incoming light and produces carriers (or electron–hole pairs). As a result, there may be a discrepancy at the intersection [27]. In an ideal PV cell model, a photocurrent source and a diode are connected in parallel. Model estimation is made easiest by the fact that there are only three unknown parameters: the ideality factor η, the photocurrent I_{pv}, and the reverse saturation current I_s.

The contact resistance R_s between the silicon and electrode surfaces is described by this resistance. A parallel resistance R_p is attached to the diode to prepare for leakage current in the PN junction. The single-diode model (SDM) model has five parameters that must be estimated: I_{pv}, I_s, R_s, and R_p [28]. The double-diode model (DDM) is a more precise method of modeling PV cells. It takes into account current loss recombination in the depletion area. With the addition of the seventh parallel diode, there are now seven parameters to estimate (I_{pv}, η_1, I_{d1}, η_2, I_{d2}, R_p, and R_s) [8].

These models are of great interest to many researchers. There have been many successful algorithms for adjusting parameters of PV cells in SDM and DDM, but few works in TDM have been published in this area. Reference [29] proposed a solar PV parameter extraction method based on the Flower Pollination Algorithm (FPA). Two diode models are chosen to understand the precision of the computation. The authors experimented with the effectiveness of FPA using RTC France info. Simulated Annealing (SA), Pattern Search (PS), Harmony Search (HS), and Artificial Bee Swarm Optimization (ABSO) techniques are often used to compare the measured root mean square error and relative error for the built model. Researchers [30] proposed a hybridized optimization algorithm (HISA) for accurately estimating the parameters of the PV cells and modules. From the experimental data obtained from five case studies consisting of two cells and three modules for monocrystalline, multi-crystalline, and thin-film PV technologies, single- and double-diode models of PV cells/modules were developed with their respective single I V nonlinear characteristics.

The authors [31] propose two simple metaphor-free algorithms called Rao-2 (R-II) and Rao-3 (R-III) to estimate the parameters of PV cells. Several well-known optimization algorithms are compared to the efficiency of the proposed algorithms. The comparison helps show the merit of the algorithms. Finally, an analysis of statistical data is combined with experimental findings to verify the efficiency of the proposed algorithms. The Grasshopper Optimization Algorithm (GOA) is proposed [32] for parameter extraction of a PV module's three-diode PV model. This GOA-based PV model uses two popular commercial modules: Kyocera KC200GT and Solarex MSX-60.

The single-, double-, and three-diode models have different solar cell parameters. These models have five parameters for the single-diode model and seven parameters for the double- and three-diode models. Each parameter must be obtained accurately based on the objective function to reach the global optimum. In this study, the EHO algorithms have been chosen to solve this problem because they have a few control parameters and smooth implementation. In addition, EHO's simplicity and few parameters made it a suitable choice for achieving such enhancements. Furthermore, by dividing the population into clans, we could avoid becoming trapped in a local optimum and instead converge on reaching a global minimum. Finally, after getting experimental results for this problem, a comparison with other well-known algorithms was presented to prove the result's quality. This comparison is important to ensure that the new variants can solve this problem and compete with other algorithms.

Table 1 reports some of the recent solvers that were applied for PV parameter estimation problems in the recent years

Table 1. Recent optimizers for PV parameter estimation.

Ref #/Year	Algorithm	Ref #/Year	Algorithm	Ref #/Year	Algorithm
[3], 2020	Projectile Search Algorithm	[32], 2020	Grasshopper Optimizer	[33], 2020	Backtracking Search Algorithm
[5], 2020	Cuckoo Search Optimizer	[34], 2020	Flower Pollination	[35], 2021	Marine Predators Optimizer
[6], 2018	Differential Evolution Algorithm	[36], 2021	Newton-Raphson jointed with Heuristic Algorithm	[37], 2020	Improved Wind-Driven Algorithm
[9], 2021	Turbulent Flow of Water Optimizer	[38], 2021	Supply–Demand Optimizer	[39], 2019	Differential Evolution Algorithm
[10], 2021	Forensic Optimizer	[40], 2021	Improved Bonobo Optimizer	[41], 2020	Slime Mold Optimizer
[11], 2021	Gorilla Optimization Algorithm	[42], 2013	Artificial Bee Swarm	[43], 2020	Coyote Optimization Algorithm
[21], 2021	Closed loop PSO and EHO	[44], 2021	Hybrid Whale and PSO Optimizer	[45], 2020	Adaptive Differential Evolution
[31], 2019	Metaphor-Less Algorithms	[46], 2021	Artificial Ecosystem Optimizer	[47], 2019	Gray Wolf Optimization

The RMSE and the relative error are used as the most performance measures developed in the previous methods. The proposed variants of EHO are compared against most of the new well-known algorithms on the parameter identification of different photovoltaics. The performance of these proposed algorithms can be judged according to convergence speed, high estimation of parameters, and low computation time.

The main contributions of this paper can be summarized as follows:

- Proposing three variants of the EHO algorithms for solar cell parameters estimation.
- The EHO and the proposed EHO variants are tested on single-, double-, and three-diode models.
- Verifying the performance of each algorithm by comparing results with those of competitors.

- Proving that the culture-based variant has the most effective performance that improves the EHO.
- Validation of the proposed variants under different environmental conditions for temperature and irradiation. In this regard, the applications are employed on two types of PV solar cells.

The rest of the paper is organized as follows. The second section focuses on solar cells and mathematical models. In Section 3, an elephant-herding algorithm is proposed, and its different versions are discussed. The results, computer simulations, and comparisons are listed and discussed in Section 4. Finally, we conclude in Section 5 with a wrap-up and conclusion.

2. Mathematical Models of Photovoltaic Cell

Solar cell models describing the I-V characteristics typically contain one diode, two diodes, or three diodes. These detailed models are described as follows:

2.1. Single Diode Model (Five-Parameter Model)

A modified Shockley diode equation can describe a single diode model. It is widely used for modeling solar cells because it is simple to implement with five parameters (I_{ph}, I_d, n, R_{sh}, R_s). However, at low illuminations, the single diode model is particularly inaccurate in describing cell behavior [48,49]. Figure 1 shows a single diode model consisting of a current source in parallel with a diode, and the module shunt resistance controls the loss of currents at the junction within the cell.

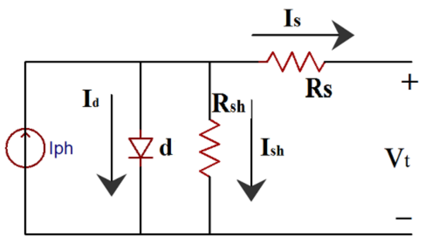

Figure 1. Single diode model.

The mathematical model of the single diode model is given by:

$$I_t = I_{ph} - I_{d1}\left[\exp\left(\frac{q(V_t + R_s \cdot I_t)}{n_1 \cdot k \cdot T}\right) - 1\right] - \frac{V_t + R_s \cdot I_t}{R_{sh}}. \quad (1)$$

2.2. Double-Diode Model (Seven-Parameter Model)

Figure 2 shows the double-diode model as an additional diode is added in parallel with the current source. This additional diode can achieve higher accuracy than a single diode model, but with seven parameters, more computation is needed (I_{ph}, I_{d1}, I_{d2}, n_1, n_2, R_{sh}, R_s).

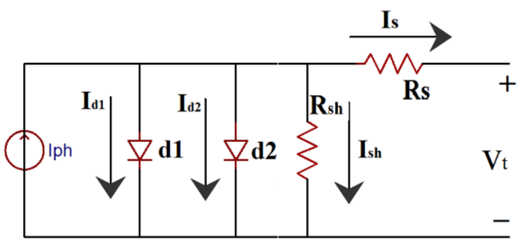

Figure 2. Double-diode model.

The mathematical model of the double-diode model is given below.

$$I_t = I_{ph} - I_{d1}\left[\exp\left(\frac{q(V_t + R_s \cdot I_t)}{n_1 \cdot k \cdot T}\right) - 1\right] - I_{d2}\left[\exp\left(\frac{q(V_t + R_s \cdot I_t)}{n_2 \cdot k \cdot T}\right) - 1\right] - \frac{V_t + R_s \cdot I_t}{R_{sh}} \quad (2)$$

2.3. Three-Diode Model (10-Parameter Model)

The three-diode model shown in Figure 3 extends the double-diode model by adding the third diode in parallel with the two other diodes. The three-diode model has three more parameters than the double-diode model (I_{d3}, n_2, K) [50,51].

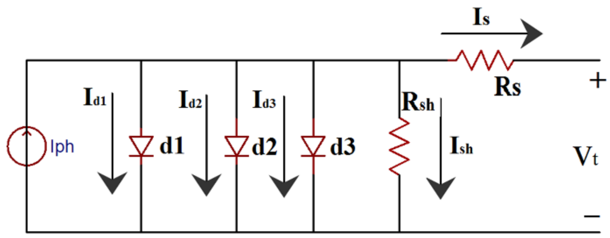

Figure 3. Three-diode model.

The mathematical formulation of the three-diode model is given by Equation (3) as:

$$I_t = I_{ph} - I_{d1}\left[\exp\left(\frac{q(V_t + R_s \cdot I_t)}{n_1 \cdot k \cdot T}\right) - 1\right] - I_{d2}\left[\exp\left(\frac{q(V_t + R_s \cdot I_t)}{n_2 \cdot k \cdot T}\right) - 1\right] - I_{d3}\left[\exp\left(\frac{q(V_t + R_s \cdot I_t)}{n_3 \cdot k \cdot T}\right) - 1\right] - \frac{V_t + R_s \cdot I_t}{R_{sh}}. \quad (3)$$

2.4. Parameter Extraction of the Solar Cell

A set of current–voltage (I–V) experimental data is given to extract the cell parameters. To define an objective function to be used in optimization algorithms, Equations (1)–(3) are reformed as in Equations (4)–(6). Equations (4)–(6) are used to get the error between the experimental and measured currents for the PV models, which are considered as the fitness functions of the three PV models.

$$f_1(V_t, I_t, y) = I_t - I_{ph} + I_{d1}\left[\exp\left(\frac{q(V_t + R_s \cdot I_t)}{n_1 \cdot k \cdot T}\right) - 1\right] + \frac{V_t + R_s \cdot I_t}{R_{sh}} \quad (4)$$

$$f_2(V_t, I_t, y) = I_t - I_{ph} + I_{d1}\left[\exp\left(\frac{q(V_t + R_s \cdot I_t)}{n_1 \cdot k \cdot T}\right) - 1\right] + I_{d2}\left[\exp\left(\frac{q(V_t + R_s \cdot I_t)}{n_2 \cdot k \cdot T}\right) - 1\right] + \frac{V_t + R_s \cdot I_t}{R_{sh}} \quad (5)$$

$$\begin{aligned} f_3(V_t, I_t, y) = I_t - I_{ph} + I_{d1}\left[\exp\left(\tfrac{q(V_t+R_s \cdot I_t)}{n_1 \cdot k \cdot T}\right) - 1\right] + I_{d2}\left[\exp\left(\tfrac{q(V_t+R_s \cdot I_t)}{n_2 \cdot k \cdot T}\right) - 1\right] \\ + I_{d3}\left[\exp\left(\tfrac{q(V_t+R_s \cdot I_t)}{n_3 \cdot k \cdot T}\right) - 1\right] + \tfrac{V_t+R_s \cdot I_t}{R_{sh}} \end{aligned} \quad (6)$$

The objective function can be implemented as the root mean square error (RMSE) as:

$$\mathrm{F} = \sqrt{\frac{1}{\mathrm{N}}\sum_{l=1}^{N} f_l(V_t, I_t, y)^2}. \quad (7)$$

3. EHO-Based Optimization Algorithms

The wild elephant grows in herds. Clans of elephants are organized into groups under the leadership of female leaders. Furthermore, male elephants abandon the herd as they mature. To implement the elephant's behavior to solve nonlinear optimization problems, EHO is summarized into three essential rules:

1. The population has a fixed number of clans; each clan consists of some elephants.
2. The male elephant separates the clan and lives alone away from the group.
3. A leadership of female elephants rules the clan.

There are clans within the elephant population, and within each clan, each elephant is ranked based on its fitness, and then each group is updated separately.

Clan updating operator: For each member in clan ci, the best elephant effect on its next position in clan *c*. We can update elephant *j* in clan *c* by:

$$x_{n,c,j} = x_{c,j} + \alpha \cdot r \cdot \left(x_{best,c} - x_{c,j}\right). \quad (8)$$

The best elephant in each clan can be updated as:

$$x_{n,c,j} = \beta \cdot x_{center,c}. \quad (9)$$

Separating operator: As mentioned, the male elephant will live alone, separately away from the family. This separating process acts as the separating operator, which can be implemented into each generation as the worst fitness. We achieve it as follows:

$$x_{worst,c} = x_{min} + r \cdot (x_{max} - x_{min} + 1). \quad (10)$$

The elephant optimization procedure has been randomly generated based on the pseudocode in Figure 4 and the flowchart in Figure 5. The EHO algorithm has significant merit of a few control parameters. However, the chances of finding a new good elephant vs. a poor one are low; thus, the new candidate solution is unlikely to be as excellent as or better than the old one. The search operator does not consider the knowledge of the best solution or other solutions that may have a beneficial influence on steering EHO toward more promising areas of search space due to the participation of these random variables. However, a closer look at the flowchart and pseudocode of EHO reveals several gaps and shortcomings. These shortcomings may have a bad impact, affecting EHO's performance.

- As depicted in Equation (10), the new generated $x_{worst\ ,ci}$ value may be worse than the original value of F. Thus, in this equation, a better value cannot be guaranteed.
- The constant value alpha (α in Equation (8)) remains consistent during algorithmic steps. Therefore, making the parameter based on the generation number of the elephant makes sense.

This paper aims to improve EHO performance, which is under-reported in the scientific literature. Listed below are three potential enhancements to EHO performance:

- Alpha tuning of αEHO.
- Cultural-based EHO (CEHO).
- Biased initialization EHO (BIEHO).

```
Initialization:
Initialize (Population size, Maximum generation, Boundaries).
Initialize the population.
Calculate the cost for each elephant.
Repeat
  Sort all population according to fitness.
  Clan updating:
  For c=1 to nClan (for each clan) do
    For j=1 to nci (for each elephant in clan c) do
      If x_c,j = x_best,ci then
          Update x_c,j (old member) and calculate x_n,c,j (new member) by Eq. (9).
      Else
          Update x_c,j (old member) and calculate x_n,c,j (new member) by Eq. (8).
      End if
    End for j
  End for c
Separating operator:
For c=1 to nClan (for each clan in population) do
    Replace the worst member in clan c by Eq. (10).
End for c
Evaluate all population by the updated elephants.
Until (Iteration = Maximum generation)
```

Figure 4. Pseudocode for EHO procedure.

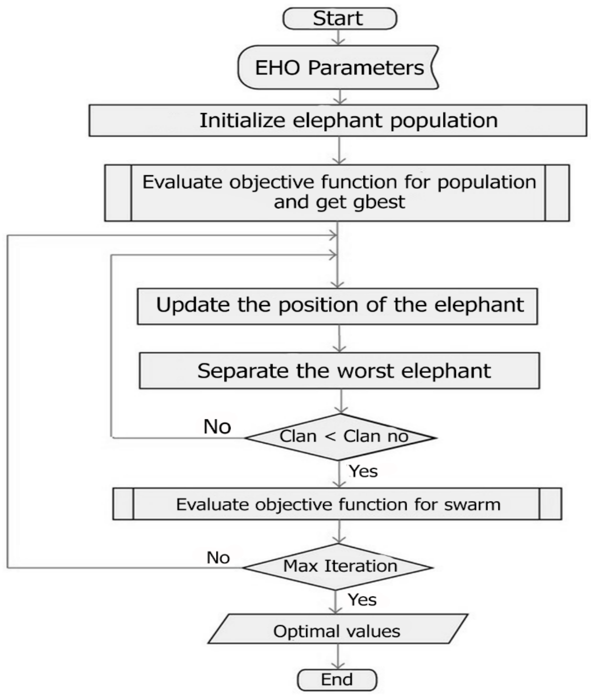

Figure 5. Flowchart of EHO.

3.1. Alpha Tuning of αEHO

Careful investigation of EHO parameters recommends setting the scale factor α to be adaptive is more promising than being a constant value in the range [0, 1].

Putting it simply, making alpha adaptive and related to the population number is more convenient and matched to the notion of evolution in Equation (11). In the original EHO algorithm, the scale factor-alpha is a constant value. Now, α is varying with the generation number by this function:

$$\alpha_{new} = \alpha + \frac{\alpha_{\max} - \alpha_{\min}}{n}. \tag{11}$$

3.2. Cultural-Based EHO (CEHO)

By utilizing the space of the best prior members, the cultural-based algorithm aids in the improvement of the algorithm [26,52,53]. The cultural-based algorithm constructs a better community by considering a belief space comprised of selected population members by acceptance function, as shown in Figure 6. A new member can be generated by using the belief space. A cultural-based algorithm is used to generate new solutions among belief space boundaries in the separating operation.

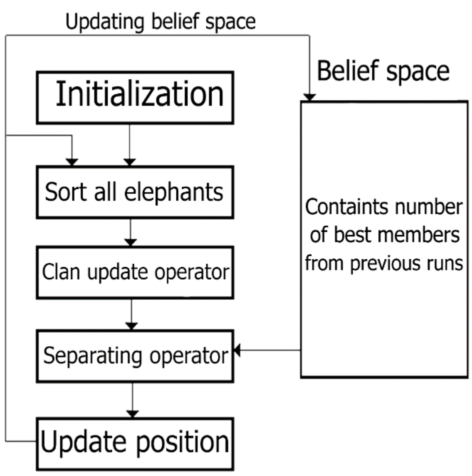

Figure 6. Belief space in cultural-based.

3.3. Biased Initialization EHO (BIEHO)

The main idea of the biased initialization algorithm is that the algorithm did not start evolving while the population's average fitness did not exceed a certain threshold. Therefore, the clan should be satisfied with its population's quality and ensure high-quality elephants. Start the generation with a population with functional fitness. The next step of evolution will not begin until the quality of the first generation reaches a suitable predetermined threshold. Biased algorithms are used in the initialization step by adding a rule or a limit [54]. Forcing the first generation of the population to have a good candidate solution may lead to another good production.

4. Computer Results and Simulations

EHO variants were tested using 57 mm diameter commercial silicon solar cells from the RTC Company of France to verify their performance against single- and double-diode models. The experiment is carried out under 1 sun (1000 W/m^2) at 33 °C [8,42,55]. A multi-crystalline PV solar module CS6P-240P is used to represent the three-diode model. CS6P-240P experimental data based on [56,57] are established for four irradiance levels (109.2, 246.65, 347.8, and 580.3 W/m^2) at temperatures (37.32, 40.05, 347.8, and 51.91 °C), respectively. Table 2 shows the manufacture specification for CS6P-240P under standard test conditions (STD). The basic EHO and its three variants are compared with the results of two algorithms from [42] called Artificial Bee Swarm Optimization algorithm (ABSO) and Harmony Search (HS) algorithm. The few adjustable parameters for EHO can be set as $\alpha = 0.9$, β = 0.1, number of clans = 4, population size = 32, and maximum iteration = 5000.

Table 2. Manufacture specification under standard test condition.

Maximum Power at STC	240 W
Optimum operating voltage	29.9 V
Optimum operating current	8.03 A
Open circuit voltage	37.0 V
Short circuit current	8.59 A
V Temperature coefficient *Voc*	−0.43%
I Temperature coefficient *Isc*	0.065%
Cell arrangement	60 (6 × 10)

Tables 3 and 4 present the optimal solar cell parameters and RMSE by EHO algorithms, Artificial Bee Swarm Optimization algorithm (ABSO), and Harmony Search (HS) for single- and double-diode modes. The single-diode model is considered the simplest model among all models with only five parameters. Table 3 shows that the four EHO algorithms obtained the same result due to the model's simplicity, but all four algorithms outperformed ABSO and HS. Table 4 shows the results for the double-diode model with seven parameters, showing differences between the extracted parameters and the RMSE. Compared to other algorithms, CEHO achieved the lowest RMSE. Figure 7 shows the convergence of the four EHO algorithms for the single-diode and double-diode model at the first 250 generations, respectively. In addition, it showed the fast convergence of the proposed EHO algorithms for obtaining good results.

Table 3. Comparison between EHO algorithms, ABS, and HS for single-diode solar cells.

Item	EHO	EHO Variants			ABSO	HS
		αEHO	CEHO	BIEHO		
I_{ph} (A)	0.76078	0.76077	0.76078	0.76077	0.7608	0.7607
I_d (μA)	0.32201	0.32143	0.32098	0.320479	0.30623	0.30495
R_s (Ω)	0.036388	0.036397	0.0364027	0.0364085	0.03659	0.03663
R_{sh} (Ω)	53.5851	53.58874	53.52479	53.49828	52.2903	53.5946
n	1.48086	1.48068	1.48054	1.48038	1.47583	1.47538
$(RMSE)$	9.861×10^{-4}	9.861×10^{-4}	9.861×10^{-4}	9.861×10^{-4}	9.9124×10^{-4}	9.9510×10^{-4}

Table 4. Comparison between EHO algorithms, ABS, and HS for double-diode solar cells.

Item	EHO	EHO Variants			ABSO	HS
		αEHO	CEHO	BIEHO		
$I_{ph}(\mathrm{A})$	0.76079	0.7607	0.76077	0.76079	0.76078	0.76176
$I_{d1}(\mu\mathrm{A})$	0.19895	0.23015	0.470885	0.294513	0.26713	0.12545
$I_{d2}(\mu\mathrm{A})$	0.25005	0.22753	0.258635	0.478734	0.38191	0.25470
$R_s(\Omega)$	0.0367292	0.036594	0.036595	0.036591	0.03657	0.03545
$R_{sh}(\Omega)$	53.47509	54.0848	54.85623	53.415705	54.6219	46.8269
$n1$	1.44596	1.45601	1.994023	1.47250	1.46512	1.49439
$n2$	1.69709	1.73558	1.462378	1.98067	1.98152	1.49989
$(RMSE)F$	9.876×10^{-4}	9.853×10^{-4}	9.830×10^{-4}	9.852×10^{-4}	9.834×10^{-4}	0.00126

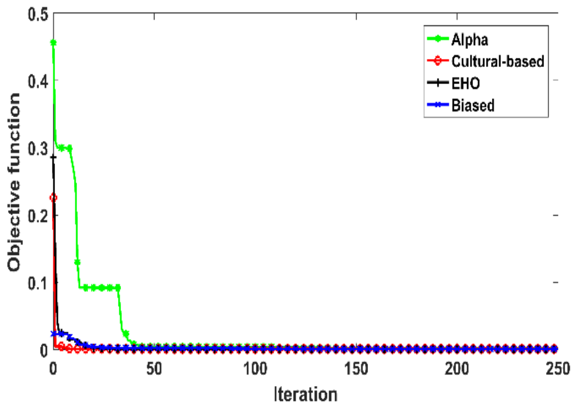

(**a**)

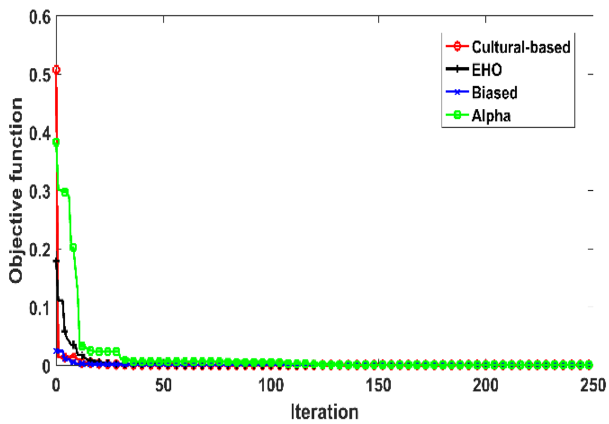

(**b**)

Figure 7. Convergence rates of EHO and its variants. (**a**) single diode. (**b**) double diode.

As demonstrated by Table 5, the measured current is very close to the calculated current. In addition, cultural-based EHO leads to outperformed results compared with other EHO variants.

Figures 8 and 9 show the power and current of the calculated and measured current from cultural-based EHO. Again, the measured and calculated curves are almost identical, while the relative error for the double-diode model for cultural-based EHO is presented in Table 6.

The previous results were for the PV panels at standard temperature and radiation. The four EHO algorithms were tested against three other algorithms at different irradiance levels and temperatures for more testing. Table 7 shows the extracted parameters for the seven algorithms at different irradiance levels and temperatures. Finally, the three-diode model is tested against three algorithms from [43] (Moth-Flame Optimizer (MFO), FPA, and Hybrid Evolutionary algorithm (DEIM)). The RMSEs for each algorithm at varying irradiance levels are listed in Table 8. Again, at low radiation with 109.2 $\mathrm{W/m^2}$, CEHO outperforms EHO with a slightly small difference but a big difference compared to other algorithms. CEHO outperformed other algorithms at other radiations, and BIEHO's results were slightly different from CEHO's. The superiority of the CEHO algorithm is proven as the best compared with the other three variants and the other three algorithms for all irradiance levels. Figure 10 shows that calculated data fit the I-V curve of measured data for CEHO.

Table 5. The relative error for 26 measurements (single diode) with CEHO.

No.	V_t (v)	I_t (A) Measured	I_{ph} (A) Calculated	Relative Error
1	−0.2057	0.764	0.764104	−0.000104
2	−0.1291	0.762	0.762674	−0.000674
3	−0.0588	0.7605	0.761362	−0.000762
4	0.0057	0.7605	0.760156	0.000344
5	0.0646	0.76	0.759053	0.000947
6	0.1185	0.759	0.758037	0.000963
7	0.1678	0.757	0.757083	−0.000083
8	0.2132	0.757	0.756130	0.00087
9	0.2545	0.7555	0.755073	0.000427
10	0.2924	0.754	0.753649	0.000351
11	0.3269	0.7505	0.751377	−0.000877
12	0.3585	0.7465	0.747342	−0.000842
13	0.3873	0.7385	0.740110	−0.000161
14	0.4137	0.728	0.727382	0.000618
15	0.4373	0.7065	0.706981	−0.000481
16	0.459	0.6755	0.675295	0.000205
17	0.4784	0.632	0.630777	0.001223
18	0.496	0.573	0.571946	0.001054
19	0.5119	0.499	0.499618	−0.000618
20	0.5265	0.413	0.413650	−0.00065
21	0.5398	0.3165	0.317502	−0.001002
22	0.5521	0.212	0.212138	−0.000138
23	0.5633	0.1035	0.102232	0.0013
24	0.5736	−0.01	−0.008728	−0.001272
25	0.5833	−0.123	−0.125504	0.002504
26	0.59	−0.21	−0.208448	−0.007552

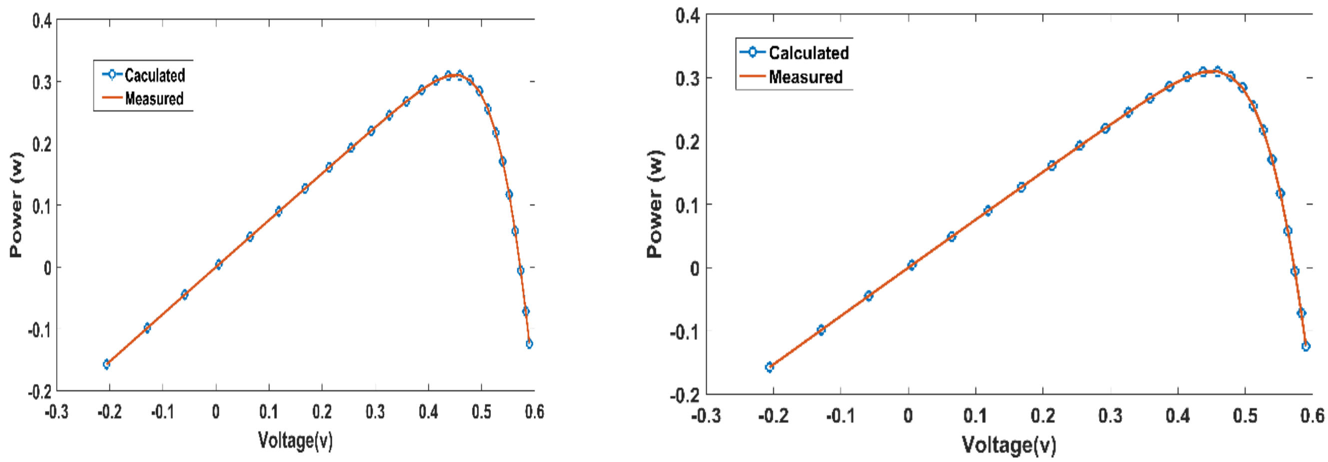

(**a**) (**b**)

Figure 8. Measured power vs. calculated by CEHO. (**a**) single diode. (**b**) double diode.

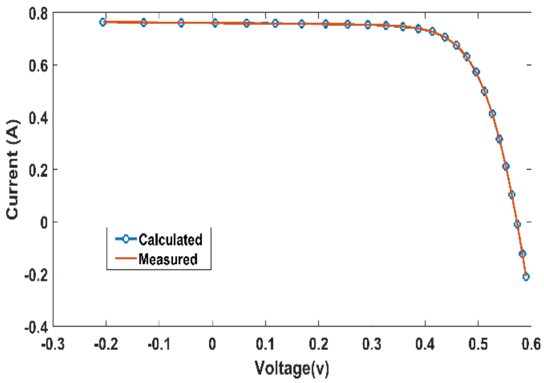

(a)

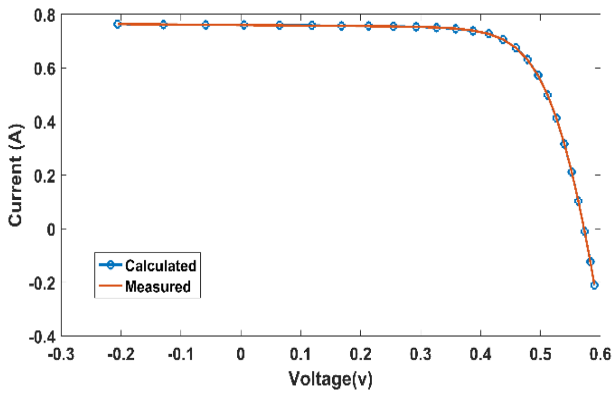

(b)

Figure 9. Measured current vs. calculated by CEHO. (**a**) single diode. (**b**) double diode.

Table 6. The relative error for 26 measurements (double diode) with CEHO.

No.	V_t (v)	I_t (A) Measured	I_{ph} (A) Calculated	Relative Error
1	−0.2057	0.764	0.764019	−0.000019
2	−0.1291	0.762	0.762623	−0.000623
3	−0.0588	0.7605	0.761343	−0.00843
4	0.0057	0.7605	0.760166	0.000334
5	0.0646	0.76	0.759088	0.006912
6	0.1185	0.759	0.758093	0.001093
7	0.1678	0.757	0.757154	−0.000154
8	0.2132	0.757	0.756208	0.000792
9	0.2545	0.7555	0.755147	0.000353
10	0.2924	0.754	0.753704	0.000296
11	0.3269	0.7505	0.751400	−0.000900
12	0.3585	0.7465	0.747325	−0.000825
13	0.3873	0.7385	0.740054	−0.001554
14	0.4137	0.728	0.727300	0.0007
15	0.4373	0.7065	0.706897	−0.000397
16	0.459	0.6755	0.675236	0.0003
17	0.4784	0.632	0.630758	0.001242
18	0.496	0.573	0.571968	0.001032
19	0.5119	0.499	0.499668	−0.000668
20	0.5265	0.413	0.413703	−0.000703
21	0.5398	0.3165	0.317536	−0.001036
22	0.5521	0.212	0.212140	−0.00014
23	0.5633	0.1035	0.102201	0.001299
24	0.5736	−0.01	−0.008761	−0.008761
25	0.5833	−0.123	−0.125531	0.002531
26	0.59	−0.21	−0.208418	−0.001582

Table 7. Comparison between different EHO algorithms among irradiance levels.

Irradiance	Algorithm	I_{ph}	I_{d1}	I_{d2}	I_{d3}	R_s	R_{sh}	n_3
580.3 W/m^2 51.91 °C	EHO	5.9992	1.7321×10^{-8}	6.7684×10^{-7}	1.1186×10^{-5}	0.39027	493.15	3.9986
	αEHO	5.9947	1.5744×10^{-8}	2.2779×10^{-7}	5.8365×10^{-5}	0.35637	4729.3	2.1169
	CEHO	5.9997	1.7336×10^{-8}	3.84148×10^{-7}	2.0015×10^{-10}	0.39055	478.607	2.7151
	BIEHO	5.9988	1.7292×10^{-8}	1.3773×10^{-6}	2.3406×10^{-8}	0.38977	502.29	3.048
	MFO	6.00066	1.7346×10^{-11}	9.210×10^{-7}	1.210×10^{-6}	0.38481	461.866	3.2135
	FBA	6.0075	1.7297×10^{-11}	8.7857×10^{-7}	9.0089×10^{-7}	0.39137	457.054	3.2926
	DEIM	6.0016	1.7363×10^{-11}	9.9751×10^{-7}	1.0234×10^{-6}	0.38524	457.282	3.2658
347.8 W/m^2 43.95 °C	EHO	3.0421	5.6398×10^{-9}	2.116×10^{-6}	2.0512×10^{-7}	0.41272	522.92	3.925
	αEHO	3.0328	4.5677×10^{-9}	7.2634×10^{-8}	3.1293×10^{-5}	0.26283	4927.8	2.001
	CEHO	3.0415	5.6216×10^{-9}	2.6116×10^{-6}	9.3642×10^{-9}	0.41118	540.79	3.9941
	BIEHO	3.0413	5.676×10^{-9}	2.1503×10^{-7}	7.9926×10^{-5}	0.41442	562.44	3.4295
	MFO	3.0457	5.6724×10^{-12}	9.985×10^{-7}	1.0234×10^{-6}	0.4163	461.524	3.2256
	FBA	3.04277	5.6211×10^{-12}	5.3506×10^{-7}	9.6777×10^{-7}	0.42925	517.401	3.1541
	DEIM	3.0454	5.6773×10^{-12}	9.9482×10^{-6}	1.3562×10^{-6}	0.41479	465.385	3.6897
246.65 W/m^2 40.05 °C	EHO	2.138	3.2543×10^{-9}	5.3294×10^{-6}	0.0005517	0.44377	4961.5	3.2946
	αEHO	2.135	2.4755×10^{-9}	9.8526×10^{-8}	4.3367×10^{-5}	0.28076	4977.9	2.0474
	CEHO	2.1379	3.2050×10^{-9}	8.1838×10^{-6}	0.0005982	0.43518	4999.86	3.4380
	BIEHO	2.1378	3.2494×10^{-9}	4.9161×10^{-6}	0.0004857	0.43959	4971.3	3.2026
	MFO	2.1435	3.3585×10^{-12}	1.62×10^{-6}	0.9391×10^{-3}	0.45333	4989.25	3.5252
	FBA	2.1484	3.453×10^{-12}	5.4342×10^{-7}	9.0503×10^{-7}	0.4923	4889.44	3.6523
	DEIM	2.1498	3.4402×10^{-12}	9.9684×10^{-7}	1.025×10^{-6}	0.8932	4746.08	3.5697
109.2 W/m^2 37.32 °C	EHO	0.99658	1.8992×10^{-9}	3.7627×10^{-7}	7.6187×10^{-7}	0.74613	469.11	3.9922
	αEHO	0.98919	1.7615×10^{-9}	6.7713×10^{-9}	3.1843×10^{-5}	0.58626	709.92	2.5034
	CEHO	0.99641	1.8939×10^{-9}	5.1732×10^{-7}	3.4151×10^{-8}	0.74203	472.73	3.8993
	BIEHO	0.99641	1.901×10^{-9}	2.5001×10^{-7}	1.8607×10^{-5}	0.74568	475.05	3.9983
	MFO	0.99853	2.2787×10^{-12}	1.0698×10^{-9}	9.9999×10^{-7}	0.7337	450.15	3.7173
	FBA	0.9978	2.2761×10^{-12}	1.0399×10^{-7}	5.8927×10^{-7}	0.7230	473.45	3.7569
	DEIM	0.9985	2.2658×10^{-12}	3.1652×10^{-8}	4.9986×10^{-7}	0.7351	449.34	3.3526

Table 8. Comparison between EHO algorithms, MFO, FBA, and DEIM for three-diode solar cells.

EHO	EHO Variants			MFO	FBA	DEIM
	αEHO	CEHO	BIEHO			
0.014598	0.026082	0.014591	0.014607	0.02455	0.02708	0.02807
0.0014236	0.02323	0.001337	0.001359	0.009927	0.016307	0.015864
0.0018575	0.006821	0.0017978	0.001821	0.012602	0.13287	0.012913
0.0009912	0.003721	0.00099094	0.0001923	0.001855	0.003607	0.0035508

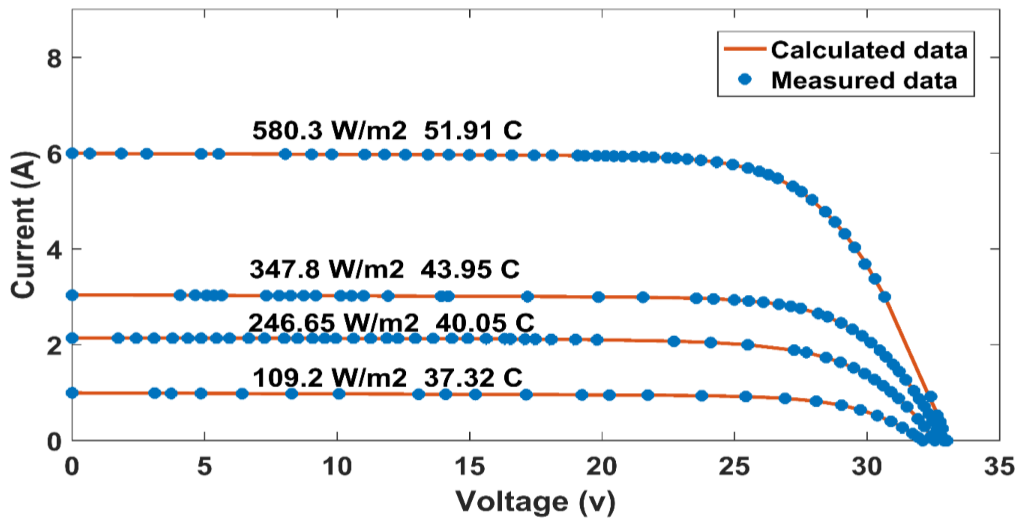

Figure 10. Measured current vs. calculated for three-diode model by CEHO.

5. Conclusions

This paper presents a new optimization algorithm based on elephant herding behavior called Elephant Herding Optimization (EHO) and three improved variants called αEHO, CEHO, and BIEHO. The EHO and its three variants are developed to estimate single, double, and three-diode solar cell models. The 57 mm diameter RTC Company of France commercial silicon solar cell with 26 points of measured data was chosen to present single and double models' problem under one irradiance level (25 °C and 1000 W/m^2). The EHO variants results are compared with two good algorithms (ABSO, HS). For presenting the three-diode model multi-crystalline PV solar module CS6P-240P under four irradiance levels (109.2, 246.65, 347.8, and 580.3 W/m^2) at temperature (37.32, 40.05, 347.8, and 51.91 °C) respectively. The EHO algorithms are compared with another three algorithms (MFO, FBA, and DEIM). The superiority of the four EHO algorithms is proven in the results. Cultural-based algorithms outperformed all algorithms used in the double- and three-diode models and ABSO, HS, and Biased in the single-diode model. Finally, it can be concluded from the results that EHO algorithms are very suitable for solving parameters extraction of solar cell problems for variant models.

Among the drawbacks of conventional EHO is its scale factor alpha being a constant value. Additionally, the behavior of EHO requires more attention to the solutions. Therefore, it would be helpful to employ more hybrid solutions, as this study recommends. Moreover, due to the practical nature of elephant herding, there are more processes involved than clan updating and separating. Thus, more models should be developed and incorporated into the EHO method that models elephant behavior. Finally, the main EHO was designed for solving continuous problems, so it must be validated for continuous and discrete problems [58].

Future work will include extracting parameters for more complex models for more accurate parameter extraction. In addition, the adaptive scaling factor is more promising than being a constant value in the range [0, 1]. Moreover, due to the superiority of the CEHO algorithm, we can do more enhancements to the CEHO algorithm to get more accurate results for more complex optimization problems. In addition, more behavior characteristics are recommended to investigate an advanced version of EHO accomplished with new hybrid algorithms.

Author Contributions: Conceptualization, Y.I.R. and M.A.E., R.A.E.-S.; methodology, A.M., A.A.M.; software, A.M., A.A.M.; validation, A.M., A.A.M.; formal analysis, M.A.E., R.A.E.-S.; investigation, A.M., A.A.M.; resources, A.M., A.A.M.; data curation, Y.I.R.; writing—original draft preparation, Y.I.R.; writing—review and editing, M.A.E., R.A.E.-S. and A.M.; visualization, A.M., A.A.M.; supervision, M.A.E., R.A.E.-S.; project administration, A.M., A.A.M. All authors have read and agreed to the published version of the manuscript.

Funding: This research received no external funding.

Institutional Review Board Statement: Not applicable.

Informed Consent Statement: Not applicable.

Data Availability Statement: Data available upon request.

Conflicts of Interest: The authors declare no conflict of interest.

Nomenclature

I_{ph}	The photogenerated current
I_d	The diode current
I_{d1}	The first diode current
I_{d2}	The second diode current
I_{d3}	The third diode current
V_t	The internal voltage
R_s	The series resistance
R_{sh}	The shunt resistance
n_1	The first diode ideality factor
n_2	The second diode ideality factor
n_3	The third diode ideality factor
k	Boltzmann's constant
T	Temperature
ql	The charge of an electron
N	Number of experimental data
$x_{n,c,j}$	Updated position for elephant j in clan c
$x_{c,j}$	Old position for elephant j in clan c
α	A scale factor ϵ [0, 1]
r	Random number ϵ [0, 1]
β	A scale factor ϵ [0, 1]
$x_{center,c}$	Centre of clan c
$x_{c,j,d}$	The d^{th} of the elephant individual $x_{c,j}$
x_{man}	Upper bound of the position of elephant
x_{min}	Lower bound of the position of elephant
$x_{worst,c}$	Worst elephant individual in clan ci
α_{min}	Lower bound of permissible range of α
α_{max}	Upper bound of permissible range of α

References

1. Ali, E.S.; El-Sehiemy, R.A.; Abou El-Ela, A.A.; Mahmoud, K.; Lehtonen, M.; Darwish, M.M.F. An effective Bi-stage method for renewable energy sources integration into unbalanced distribution systems considering uncertainty. *Processes* **2021**, *9*, 471. [CrossRef]
2. Haider, H.T.; See, O.H.; Elmenreich, W. A review of residential demand response of smart grid. *Renew. Sustain. Energy Rev.* **2016**, *59*, 166–178. [CrossRef]
3. Shahabuddin, M.; Asim, M.; Sarwar, A. Parameter Extraction of a Solar PV Cell Using Projectile Search Algorithm. In Proceedings of the 2020 International Conference on Advances in Computing, Communication Materials (ICACCM), Dehradun, India, 21–22 August 2020; pp. 357–361.
4. El-Sayed, M.M.; Abou El-Ela, A.A.; El-Sehiemy, R.A. Effect of photovoltaic system on power quality in electrical distribution networks. In Proceedings of the 2016 18th International Middle-East Power Systems Conference, MEPCON 2016—Proceedings, Cairo, Egypt, 27–29 December 2017; pp. 1005–1012.
5. Gude, S.; Jana, K.C. Parameter extraction of photovoltaic cell using an improved cuckoo search optimization. *Sol. Energy* **2020**, *204*, 280–293. [CrossRef]
6. Chellaswamy, C.; Ramesh, R. Parameter extraction of solar cell models based on adaptive differential evolution algorithm. *Renew. Energy* **2016**, *97*, 823–837. [CrossRef]
7. Ali, S. New method for computing single diode model parameters of photovoltaic modules. *Renew. Energy* **2018**, *128*, 30–36. [CrossRef]
8. Chenouard, R.; El-Sehiemy, R.A. An interval branch and bound global optimization algorithm for parameter estimation of three photovoltaic models. *Energy Convers. Manag.* **2020**, *205*, 112400. [CrossRef]
9. Said, M.; Shaheen, A.M.; Ginidi, A.R.; El-Sehiemy, R.A.; Mahmoud, K.; Lehtonen, M.; Darwish, M.M.F. Estimating Parameters of Photovoltaic Models Using Accurate Turbulent Flow of Water Optimizer. *Processes* **2021**, *9*, 627. [CrossRef]
10. El-Sehiemy, R.A.; Shaheen, A.M.; Ginidi, A.; Sherif, S.M. Ghoneim A Forensic-Based Investigation Algorithm for Parameter Extraction of Solar Cell models. *IEEE Access* **2020**, *205*, 112400. [CrossRef]

11. Ginidi, A.; Ghoneim, S.M.; Elsayed, A.; El-Sehiemy, R.; Shaheen, A.; El-Fergany, A. Gorilla Troops Optimizer for Electrically Based Single and Double-Diode Models of Solar Photovoltaic Systems. *Sustainability* **2021**, *13*, 9459. [CrossRef]
12. Lun, S.X.; Wang, S.; Yang, G.H.; Guo, T.T. A new explicit double-diode modeling method based on Lambert W-function for photovoltaic arrays. *Sol. Energy* **2015**, *116*, 69–82. [CrossRef]
13. AlRashidi, M.R.; AlHajri, M.F.; El-Naggar, K.M.; Al-Othman, A.K. A new estimation approach for determining the I–V characteristics of solar cells. *Sol. Energy* **2011**, *85*, 1543–1550. [CrossRef]
14. Khalik, M.A.; Sherif, M.; Saraya, S.; Areed, F. Parameter identification problem: Real-coded GA approach. *Appl. Math. Comput.* **2007**, *187*, 1495–1501. [CrossRef]
15. Ishaque, K.; Salam, Z.; Mekhilef, S.; Shamsudin, A. Parameter extraction of solar photovoltaic modules using penalty-based differential evolution. *Appl. Energy* **2012**, *99*, 297–308. [CrossRef]
16. Askarzadeh, A.; Rezazadeh, A. Parameter identification for solar cell models using harmony search-based algorithms. *Sol. Energy* **2012**, *86*, 3241–3249. [CrossRef]
17. Oliva, D.; Cuevas, E.; Pajares, G. Parameter identification of solar cells using artificial bee colony optimization. *Energy* **2014**, *72*, 93–102. [CrossRef]
18. El-Naggar, K.M.; AlRashidi, M.R.; AlHajri, M.F.; Al-Othman, A.K. Simulated annealing algorithm for photovoltaic parameters identification. *Sol. Energy* **2012**, *86*, 266–274. [CrossRef]
19. Elsakaan, A.A.; El-Sehiemy, R.A.; Kaddah, S.S.; Elsaid, M.I. An enhanced moth-flame optimizer for solving non-smooth economic dispatch problems with emissions. *Energy* **2018**, *157*, 1063–1078. [CrossRef]
20. Rizk-Allah, R.M.; El-Sehiemy, R.A.; Wang, G.-G. A novel parallel hurricane optimization algorithm for secure emission/economic load dispatch solution. *Appl. Soft Comput.* **2017**, *63*, 206–222. [CrossRef]
21. Bayoumi, A.S.; El-Sehiemy, R.A.; Mahmoud, K.; Lehtonen, M.; Darwish, M.M.F. Assessment of an improved three-diode against modified two-diode patterns of MCS solar cells associated with soft parameter estimation paradigms. *Appl. Sci.* **2021**, *11*, 1055. [CrossRef]
22. Meena, N.K.; Parashar, S.; Swarnkar, A.; Gupta, N.; Niazi, K.R. Improved Elephant Herding Optimization for Multiobjective DER Accommodation in Distribution Systems. *IEEE Trans. Ind. Inf.* **2018**, *14*, 1029–1039. [CrossRef]
23. Zaky, A.A.; El Sehiemy, R.A.; Rashwan, Y.I.; Elhossieni, M.A.; Gkini, K.; Kladas, A.; Falaras, P. Optimal Performance Emulation of PSCs using the Elephant Herd Algorithm Associated with Experimental Validation. *ECS J. Solid State Sci. Technol.* **2019**, *8*, Q249–Q255. [CrossRef]
24. Zaky, A.A.; Ibrahim, M.N.; Rezk, H.; Christopoulos, E.; El Sehiemy, R.A.; Hristoforou, E.; Kladas, A.; Sergeant, P.; Falaras, P. Energy efficiency improvement of water pumping system using synchronous reluctance motor fed by perovskite solar cells. *Int. J. Energy Res.* **2020**. [CrossRef]
25. Wang, G.G.; Deb, S.; Gao, X.Z.; Dos Santos Coelho, L. A new metaheuristic optimisation algorithm motivated by elephant herding behaviour. *Int. J. Bio-Inspired Comput.* **2016**, *8*, 394–409. [CrossRef]
26. Elhosseini, M.A.; El Sehiemy, R.A.; Rashwan, Y.I.; Gao, X.Z. On the performance improvement of elephant herding optimization algorithm. *Knowl.-Based Syst.* **2019**, *166*, 58–70. [CrossRef]
27. Chin, V.J.; Salam, Z.; Ishaque, K. Cell modelling and model parameters estimation techniques for photovoltaic simulator application: A review. *Appl. Energy* **2015**, *154*, 500–519. [CrossRef]
28. Bai, J.; Liu, S.; Hao, Y.; Zhang, Z.; Jiang, M.; Zhang, Y. Development of a new compound method to extract the five parameters of PV modules. *Energy Convers. Manag.* **2014**. [CrossRef]
29. Alam, D.F.; Yousri, D.A.; Eteiba, M.B. Flower pollination algorithm based solar PV parameter estimation. *Energy Convers. Manag.* **2015**, *101*, 410–422. [CrossRef]
30. Kler, D.; Goswami, Y.; Rana, K.P.S.; Kumar, V. A novel approach to parameter estimation of photovoltaic systems using hybridized optimizer. *Energy Convers. Manag.* **2019**, *187*, 486–511. [CrossRef]
31. Premkumar, M.; Babu, T.S.; Umashankar, S.; Sowmya, R. A new metaphor-less algorithms for the photovoltaic cell parameter estimation. *Optik* **2020**, *208*, 164559. [CrossRef]
32. Elazab, O.S.; Hasanien, H.M.; Alsaidan, I.; Abdelaziz, A.Y.; Muyeen, S.M. Parameter estimation of three diode photovoltaic model using grasshopper optimization algorithm. *Energies* **2020**, *13*, 497. [CrossRef]
33. Zhang, Y.; Jin, Z.; Zhao, X.; Yang, Q. Backtracking search algorithm with Lévy flight for estimating parameters of photovoltaic models. *Energy Convers. Manag.* **2020**, *208*, 112615. [CrossRef]
34. Oliva, D.; Elaziz, M.A.; Elsheikh, A.H.; Ewees, A.A. A review on meta-heuristics methods for estimating parameters of solar cells. *J. Power Sources* **2019**, *435*, 126683. [CrossRef]
35. Bayoumi, A.S.A.; El-Sehiemy, R.A.; Abaza, A. Effective PV Parameter Estimation Algorithm Based on Marine Predators Optimizer Considering Normal and Low Radiation Operating Conditions. *Arab. J. Sci. Eng.* **2021**. [CrossRef]
36. Gnetchejo, P.J.; Ndjakomo Essiane, S.; Dadjé, A.; Ele, P. A combination of Newton-Raphson method and heuristics algorithms for parameter estimation in photovoltaic modules. *Heliyon* **2021**, *7*, e06673. [CrossRef]
37. Ibrahim, I.A.; Hossain, M.J.; Duck, B.C.; Nadarajah, M. An improved wind driven optimization algorithm for parameters identification of a triple-diode photovoltaic cell model. *Energy Convers. Manag.* **2020**, *213*, 112872. [CrossRef]
38. Ginidi, A.R.; Shaheen, A.M.; El-Sehiemy, R.A.; Elattar, E. Supply demand optimization algorithm for parameter extraction of various solar cell models. *Energy Rep.* **2021**, *7*, 5772–5794. [CrossRef]

39. Chin, V.J.; Salam, Z. A New Three-point-based Approach for the Parameter Extraction of Photovoltaic Cells. *Appl. Energy* **2019**, *237*, 519–533. [CrossRef]
40. Abdelghany, R.Y.; Kamel, S.; Sultan, H.M.; Khorasy, A.; Elsayed, S.K.; Ahmed, M. Development of an Improved Bonobo Optimizer and Its Application for Solar Cell Parameter Estimation. *Sustainability* **2021**, *13*, 3863. [CrossRef]
41. Kumar, C.; Raj, T.D.; Premkumar, M.; Raj, T.D. A new stochastic slime mould optimization algorithm for the estimation of solar photovoltaic cell parameters. *Optik* **2020**, *223*, 165277. [CrossRef]
42. Askarzadeh, A.; Rezazadeh, A. Artificial bee swarm optimization algorithm for parameters identification of solar cell models. *Appl. Energy* **2013**, *102*, 943–949. [CrossRef]
43. Chin, V.J.; Salam, Z. Coyote optimization algorithm for the parameter extraction of photovoltaic cells. *Solar Energy* **2019**, *194*, 656–670. [CrossRef]
44. Rezk, H.; Babu, T.S.; Al-Dhaifallah, M.; Ziedan, H.A. A robust parameter estimation approach based on stochastic fractal search optimization algorithm applied to solar PV parameters. *Energy Rep.* **2021**, *7*, 620–640. [CrossRef]
45. Naraharisetti, J.N.L.; Devarapalli, R.; Bathina, V. Parameter extraction of solar photovoltaic module by using a novel hybrid marine predators–success history based adaptive differential evolution algorithm. *Energy Sources Part A Recover. Util. Environ. Eff.* **2020**, 1–23. [CrossRef]
46. El-Dabah, M.A.; El-Sehiemy, R.A.; Becherif, M.; Ebrahim, M.A. Parameter estimation of triple diode photovoltaic model using an artificial ecosystem-based optimizer. *Int. Trans. Electr. Energy Syst.* **2021**, e13043. [CrossRef]
47. Nayak, B.; Mohapatra, A.; Mohanty, K.B. Parameter estimation of single diode PV module based on GWO algorithm. *Renew. Energy Focus* **2019**, *30*, 1–12. [CrossRef]
48. Ghani, F.; Duke, M. Numerical determination of parasitic resistances of a solar cell using the Lambert W-function. *Sol. Energy* **2011**, *85*, 2386–2394. [CrossRef]
49. Macabebe, E.Q.B.; Sheppard, C.J.; van Dyk, E.E. Parameter extraction from I–V characteristics of PV devices. *Sol. Energy* **2011**, *85*, 12–18. [CrossRef]
50. Khanna, V.; Das, B.K.; Bisht, D.; Singh, P.K. A three diode model for industrial solar cells and estimation of solar cell parameters using PSO algorithm. *Renew. Energy* **2015**, *78*, 105–113. [CrossRef]
51. Laudani, A.; Riganti Fulginei, F.; de Castro, F.; Salvini, A. Irradiance intensity dependence of the lumped parameters of the three-diodes model for organic solar cells. *Sol. Energy* **2018**, *163*, 526–536. [CrossRef]
52. Haikal, A.; Elhosseini, M. Modified cultural-based genetic algorithm for process optimization. *Ain Shams Eng. J.* **2011**, *2*, 173–182. [CrossRef]
53. Daneshyari, M.; Yen, G.G. Cultural-Based Multiobjective Particle Swarm Optimization. *IEEE Trans. Syst. Man Cybern. Part B* **2011**, *41*, 553–567. [CrossRef]
54. Ruiz, E.; Soto-Mendoza, V.; Ruiz Barbosa, A.E.; Reyes, R. Solving the open vehicle routing problem with capacity and distance constraints with a biased random key genetic algorithm. *Comput. Ind. Eng.* **2019**, *133*, 207–219. [CrossRef]
55. Liu, Y.; Chong, G.; Heidari, A.A.; Chen, H.; Liang, G.; Ye, X.; Cai, Z.; Wang, M. Horizontal and vertical crossover of Harris hawk optimizer with Nelder-Mead simplex for parameter estimation of photovoltaic models. *Energy Convers. Manag.* **2020**, *223*. [CrossRef]
56. Stropnik, R.; Stritih, U. Increasing the efficiency of PV panel with the use of PCM. *Renew. Energy* **2016**, *97*, 671–679. [CrossRef]
57. Islam, M.A.; Merabet, A.; Beguenane, R.; Ibrahim, H. Modeling solar photovoltaic cell and simulated performance analysis of a 250W PV module. In Proceedings of the 2013 IEEE Electrical Power Energy Conference, Halifax, NS, Canada, 21–23 August 2013; pp. 1–6.
58. Li, W.; Wang, G.-G.; Alavi, A.H. Learning-based elephant herding optimization algorithm for solving numerical optimization problems. *Knowl.-Based Syst.* **2020**, *195*, 105675. [CrossRef]